January 2012

Mapping lava flows from Nyamuragira volcano (1967-2011) with satellite data and automated classification methods

Elisabet Head
Eastern Illinois University, emhead@eiu.edu

Ann L. MacLean
Michigan Technological University

Simon A. Carn
Michigan Technological University

Geomatics, Natural Hazards and Risk
2012, 1–26, i*First* article

Taylor & Francis
Taylor & Francis Group

Mapping lava flows from Nyamuragira volcano (1967–2011) with satellite data and automated classification methods

ELISABET M. HEAD[†], ANN L. MACLEAN[‡] and SIMON A. CARN[†]
[†]Department of Geological and Mining Engineering and Sciences, Michigan Technological University, Houghton, MI 49931, USA
[‡]School of Forest Resources and Environmental Science, Michigan Technological University, Houghton, MI 49931, USA

(*Received 3 September 2011; in final form 26 March 2012*)

The volume, location and extent of historical lava flows are important when assessing volcanic hazards, as well as the productivity or longevity of a volcanic system. We use a Landsat/Hyperion/ALI dataset and automated classification methods to map lava flows at Nyamuragira volcano (1967–2011) in the Democratic Republic of the Congo. The humid tropical climate of Nyamuragira is advantageous because its lava flows are emplaced onto heavily forested flanks, resulting in strong contrast between lava and vegetation, which contributes to efficient flow mapping. With increasing age, there is an increase in Landsat band-4 reflectance, suggesting lava flow revegetation with time. This results in a distinct spectral contrast to delineate overlapping flows emplaced ~5 years apart. Areal extents of the flows are combined with published lava flow thicknesses to derive volumes. The Landsat/Hyperion/ALI dataset is advantageous for mapping future flows quickly and inexpensively, particularly for volcano observatories where resources are limited.

1. Introduction

1.1. Lava flow mapping

Mapping lava flows from volcanic eruptions serves many purposes, such as the determination of vent locations, the areal extents of flows (widths and lengths), and flow volumes. Knowledge of the geographical position and direction of flows is used in hazard prediction (Trusdell 1995). Lava volumes can be estimated through either a combination of lava flow area with field-based lava flow thickness measurements (Shaw and Swanson 1970; Self *et al.* 1997; Crown and Baloga 1999) or subtraction of pre- and post-eruptive digital elevation models (DEMs) (Rowland *et al.* 2003; Lu *et al.* 2004). These volumes can be used in magma supply models and time-series analyses of volcanic activity to further the understanding of eruption mechanisms (Burt *et al.* 1994). At volcanoes situated in remote or politically unstable locations where ground-based monitoring and fieldwork are hazardous or impossible, airborne and spaceborne remote sensing techniques are particularly useful (Abrams *et al.* 1991; Harris *et al.* 1999; Carn and Oppenheimer 2000; Carn *et al.* 2003; Patrick *et al.* 2003). For Nyamuragira volcano in the Democratic Republic of the Congo (D.R. Congo), this is

*Corresponding author. Email: emhead@mtu.edu

Geomatics, Natural Hazards and Risk
ISSN 1947-5705 Print/ISSN 1947-5713 Online © 2012 Taylor & Francis
http://www.tandf.co.uk/journals
http://dx.doi.org/10.1080/19475705.2012.680503

certainly the case. Not only is Nyamuragira's lava flow field remote, it is also extensive (figure 1), and persistent insecurity in the region continues to preclude detailed field surveys of the entire flow field. Therefore, remote sensing has proven to be a crucial tool to investigate Nyamuragira's eruptive behaviour (Carn and Bluth 2003; Colclough 2005; Bluth and Carn 2008; Smets et al. 2010).

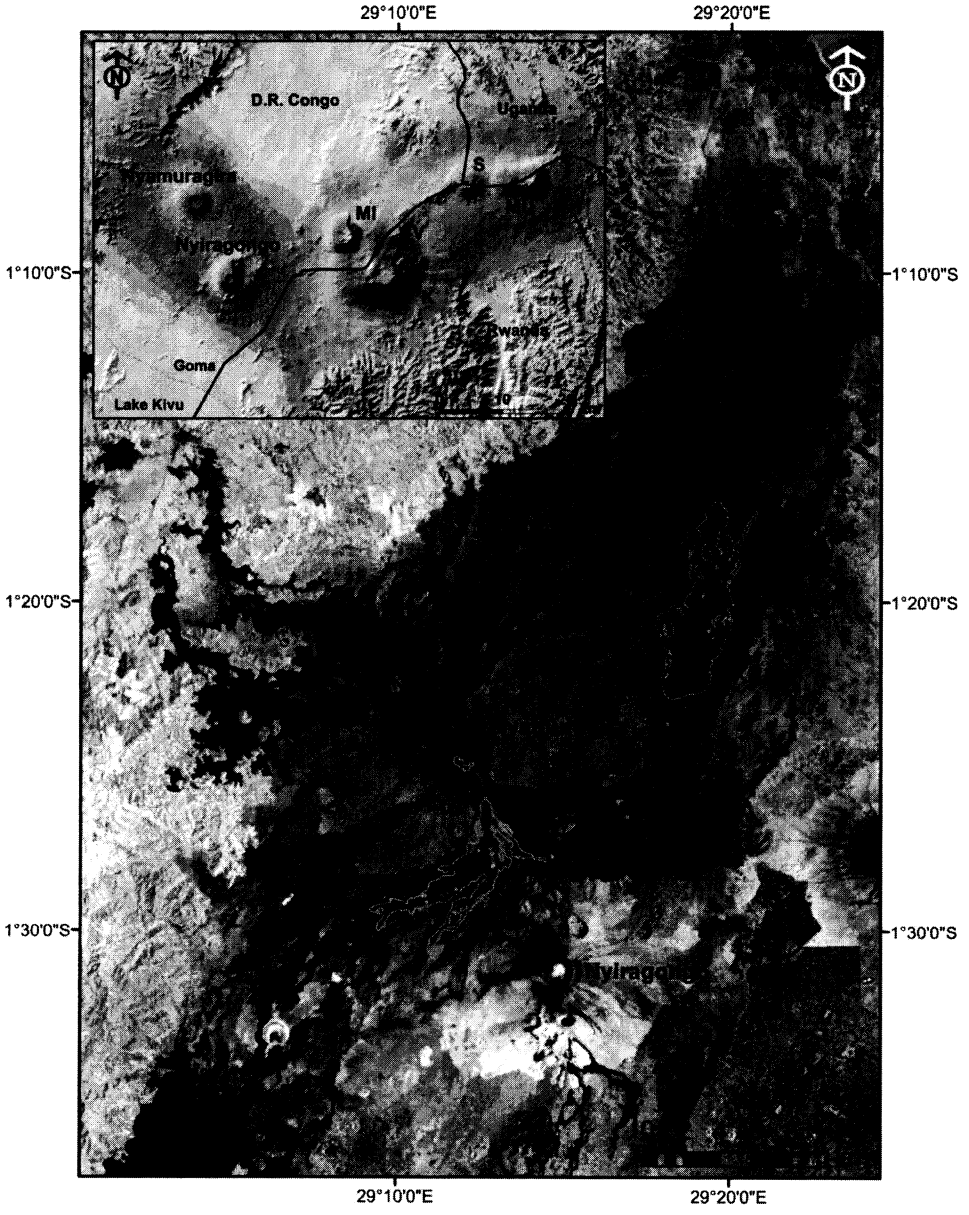

Figure 1. The inset map, an ASTER GDEM, shows the location of Nyamuragira (D.R. Congo) within the western branch of the East African Rift near the Rwandan border. Inactive Virunga volcanoes are shown: K-Karisimbi; Mi-Mikeno; S-Sabinyo; V-Visoke; Mu-Muhavara. The larger Landsat image, acquired 21 February 2005 (band 4), reveals Nyamuragira's prolific lava flows including outlines of the 2006, 2010 and 2011 flows we mapped using automated classification.

1.2. *Volcanic activity at Nyamuragira*

The western branch of the East African Rift can be divided into four volcanic provinces from north to south: (1) Toro-Ankole in western Uganda, (2) Virunga and (3) Kivu spanning the D.R. Congo, Rwanda, Burundi, and southern Uganda and (4) the Rungwe in southern Tanzania (Kampunzu *et al.* 1998; Ebinger and Furman 2002). Nyamuragira (also known as Nyamulagira; 1.41°S, 29.20°E) and its neighbouring volcano, Nyiragongo, are part of the Virunga volcanic chain and are the only active volcanoes in the western branch (figure 1). The currently inactive Virunga volcanoes are Muhavara, Sabinyo, Visoke, Mikeno and Karisimbi.

Nyamuragira erupted 16 times between 1980 and 2011, making it one of the world's most active and productive volcanoes (Smithsonian, Institution, monthly reports, 1971–2011, http://www.volcano.si.edu/world/volcano.cfm?vnum=0203-02=&vol page=var, hereinafter referred to as Smithsonian Institution, monthly reports, 1971–2011 (e.g. Smithsonian Institution 1971–2011)). A shield volcano with a near-circular summit caldera measuring 2×2.3 km at an elevation of ~ 3 km, Nyamuragira produces low-silica, high alkali lava compositions (SiO_2 ranging from 43 to 56 wt.%; $NaO + K_2O$ up to 7 wt.%), which have reached flow rates of up to ~ 20 km/h (Aoki *et al.* 1985; Hayashi *et al.* 1992; Smithsonian Institution 1971–2011). Based on reports from the Smithsonian's Global Volcanism Network (GVN; Smithsonian Institution 1971–2011), most of Nyamuragira's eruptive history has consisted of summit (intra-caldera) and effusive flank eruptions. Nyamuragira eruptions typically begin with ~ 200 m high fire fountains and contemporaneous lava flows. Tephra fall is commonly reported during Nyamuragira eruptions, and ash from several eruptions has been associated with destruction of crops and health problems in the surrounding area (Smithsonian Institution 1971–2011).

1.3. *History of Nyamuragira lava flow mapping*

Thonnard *et al.* (1965) produced a map showing Nyamuragira lava flows erupted until 1958. Kasahara *et al.* (1991) compiled published volumes from several sources for individual eruptions between 1900 and 1991, although no lava flow map was created. Since 1994, political unrest in the D.R. Congo has prohibited not only ground-based mapping efforts, but also most ground-based volcano monitoring of Nyamuragira (e.g. volcanic gas measurements, levelling surveys) from the Goma Volcano Observatory. Therefore, satellite observations have been essential for post-1994 studies of volcanic activity in the Virunga. Satellite-based radar mapping efforts were carried out for individual flows and cones from Nyamuragira (Mackay and Mouginis-Mark 1997; Colclough 2005), Nyiragongo (Mackay and Mouginis-Mark 1997; Colclough 2005), and Karisimbi (Mackay and Mouginis-Mark 1997). A more recent study by Smets *et al.* (2010) utilized radar data and optical imagery, and the Thonnard *et al.* (1965) map, to manually trace lava flow boundaries and map Nyamuragira lava flows erupted between 1938 and 2010. Herein, we apply automated classification methods to Landsat data, with the addition of Hyperion and ALI data when cloud-free Landsat scenes were unavailable, to map lava flows erupted from Nyamuragira between 1967 and 2011. We describe the image processing techniques used to delineate the lava flows, and compare our results with prior Nyamuragira mapping efforts (Colclough 2005; Smets *et al.* 2010).

As cloud cover can hinder satellite-based lava flow mapping using optical datasets, it is best to utilize satellite data from a variety of sources, collected on a range of days. Combining high spatial resolution aerial photography with medium-to-high spatial resolution optical, thermal (temperature) and radar (textural) satellite data would be optimal, as it would allow a more complete characterization of the lava flows, although high spatial resolution data can be prohibitively expensive for resource-limited volcano observatories. For our mapping efforts, we assessed the use of aerial photographs, which have been used in the past to aid lava flow mapping (Ray 1960; Abrams *et al.* 1996; Legeley-Pandovani *et al.* 1997). However, historical photography has been poorly preserved for Nyamuragira. Aerial photography of the Nyamuragira lava flow field with little or no metadata only exists up to the 1950s (B. Smets pers. comm.), while new orthographic aerial photography is difficult to obtain due to the current political climate. In contrast, remotely sensed satellite imagery is readily available.

Since radar can penetrate cloud cover, it is a useful tool in tropical regions such as Nyamuragira where cloud cover is significant (e.g. Carn 1999). Satellite-based radar imagery has been used to map Nyamuragira's lava flows (Colclough 2005; Smets *et al.* 2010), although Colclough (2005), who attempted mapping of the 1998 and 2001 Nyamuragira flows, points out that radar prohibited the mapping of all downslope flow sections. Colclough (2005) used 11 ERS 1/ERS 2 synthetic aperture radar (SAR) images acquired between 1997 and 2003, and compared the backscattered energy between SAR pairs to assess changes over time, such as the emplacement of new lava flows. The 1998 and 2001 flows were emplaced on top of older flows downslope, all of which produced a similar backscattering signal in the 5.66 cm (C-band) wavelength, preventing the separation (delineation of boundaries) between the fresh and older flows. Colclough (2005) used optical satellite data to supplement and/or verify the ambiguous flow boundaries resulting from the radar imagery. Smets *et al.* (2010) used individual SAR images and SAR pairs from ERS 1/ ERS 2 (C-band), ENVISAT (C-band) and JERS (L-band: 23.5 cm) satellites for the purpose of delineating overlapping lava flows near the summit through textural differences between flows. However, they make it clear that a combination of radar and optical imagery was necessary. In this study, we focus on an optical satellite dataset, since these data are more readily available than radar for routine mapping efforts.

Optical satellite data are often free and have been used to map lava flows utilizing various approaches (Abrams *et al.* 1991, 1996; Kahle *et al.* 1995; Lu *et al.* 2004), including on-screen digitising (tracing) of lava flow boundaries and automated classification using supervised and unsupervised algorithms. Automated classification, performed via image processing software, evaluates every pixel in a scene and then groups the pixels with similar values (e.g. digital number, reflectance, radiance) into a specified number of classes. Image processing software can be costly, although freeware exists (e.g. MultiSpec: https://engineering.purdue.edu/~biehl/MultiSpec/; GRASS GIS: http://grass.-fbk.eu/), which would allow a volcano observatory with limited funds to carry out unsupervised classification and digitization on optical satellite data. Here, we use automated classification methods with Landsat multi-spectral scanner (MSS), thematic mapper (TM) and enhanced thematic mapper (ETM+), and Earth Observing-1 (EO-1) Hyperion and Advanced Land Imager (ALI) imagery to delineate lava flows from Nyamuragira volcano.

One of the advantages of Nyamuragira's humid tropical location is that its lava flows are usually emplaced onto heavily forested flanks, resulting in strong contrast between lava and vegetation, typically allowing rapid and automated mapping. Visible to short-wave infrared (VSWIR) satellite imagery, therefore, proved optimal for mapping the Nyamuragira lava flow field. This was our main motivation for choosing the Landsat-Hyperion-ALI dataset. These data have a low cost (most data are now free) and the Landsat data in particular provide a longer-term archive (beginning in 1972) relative to other VSWIR sensors such as the advanced spaceborne thermal emission and reflection radiometer (ASTER), the Indian remote sensing satellites and Système Pour l'Observation de la Terre (SPOT). An additional advantage is that the free dataset and processing software would allow researchers or observatories in developing countries with limited resources to efficiently update the map when new lava flows occur. Due to the lack of a cloud-free Landsat scene for mapping the 2010 and 2011 flows, we used Hyperion and ALI images, respectively. We show that our area and volume estimates agree well with the estimates of Smets *et al.* (2010), which suggests that the methods we used with free satellite imagery are promising and cost-effective for Nyamuragira, as well as for similar lava flows on other volcanoes.

2. Data acquisition and mapping methodologies

2.1. Data preparation

The specifications and characteristics of the Landsat MSS, TM and ETM+, Hyperion, and ALI scenes obtained for mapping are given in tables 1 and 2, respectively. For consistency, our original intent was to use only Landsat data, but the clearest Landsat image of the 2010 flow available to date (18 January 2010) was acquired while the volcano was still erupting. An eruption cloud obstructed part of the flow and the northern-most vent was issuing hot lava, which saturated the SWIR bands. The application of automated processing techniques was not possible due to these effects. In place of Landsat, we used a Hyperion scene acquired on 28 May 2010 to complete the 2010 mapping. For the 2011 flow, we had similar problems. The eruption began on 6 November 2011 and it is still continuing at the time of writing. Current activity includes lava flows and occasional Strombolian eruptions, although at a lower level of intensity than previously observed. A cloud-free Landsat scene (acquired on 9 February 2012) does exist, but it captured the erupting lava flows, which saturated the SWIR bands and prevented automated processing. In place of this Landsat scene, we used an ALI image acquired on 3 January 2012. Since Nyamuragira was degassing during the ALI acquisition, eruption clouds did obstruct a small southern portion of the flow in this image. However, we were able to use the Landsat scene from 9 February to make minor modifications to the flow once the automated classification was performed on the ALI image.

The Hyperion image was acquired $\sim$3 months after the 2010 flow emplacement, and the ALI image was acquired $\sim$1 month after the 2011 eruption began, which preserved a good contrast between the fresh 2010/2011 lava flows and the surrounding older lava flows and vegetation. For the Landsat dataset, images acquired closest to the date of flow emplacement were used to map that particular flow. This ensured the largest contrast between fresh lava flow and surrounding vegetation and/or older, weathered lava flows. For example, the 1986 Landsat image

Table 1. Specifications of Landsat, Hyperion and ALI sensors.

	Landsat MSS	Landsat TM	Landsat ETM+	Hyperion	ALI
Dates of operation; sensor	1972–1983; 1–3	July 1982-Nov 2011, 4–5	April 1999-present, 7	Nov 2000-present	Nov 2000-present
Spectral bands	Band 4/1 (0.5–0.6 μm) Band 5/2 (0.6–0.7 μm) Band 6/3 (0.7–0.8 μm) Band 7/4 (0.8–1.1 μm)	Band 1 (0.45–0.52 μm) Band 2 (0.52–0.60 μm) Band 3 (0.63–0.69 μm) Band 4 (0.76–0.90 μm) Band 5 (1.55–1.75 μm) Band 7 (2.08–2.35 μm)	Band 1 (0.45–0.52 μm) Band 2 (0.52–0.60 μm) Band 3 (0.63–0.69 μm) Band 4 (0.77–0.90 μm) Band 5 (1.55–1.75 μm) Band 7 (2.09–2.35 μm)	Bands 41–76 (0.76–0.90 μm)	Band 1′ (0.43–0.45 μm) Band 1 (0.45–0.52 μm) Band 2 (0.53–0.61 μm) Band 3 (0.63–0.69 μm) Band 4 (0.78–0.81 μm) Band 4′ (0.85–0.89 μm) Band 5′ (1.2–1.3 μm) Band 5 (1.55–1.75 μm) Band 7 (2.08–2.35 μm)
Spatial resolution	80 m (all bands)	30 m (bands 1–5 and 7: visible, near infrared, and short wave infrared)	30 m (bands 1–5 and 7: visible, near infrared, and short wave infrared)	30 m (all bands)	30 m (bands 1′–7; visible, near infrared, and short wave infrared)
Temporal resolution	16–18 days	16 days	16 days	16 days	16 days

Table 2. Landsat, Hyperion, and ALI scenes used to map Nyamuragira lava flows. GloVis is a USGS web site from which optical satellite imagery can be downloaded (http://glovis.usgs.gov/).

Scene	Date of acquisition	Image ID (Path: 173, Row: 61)	Source
Landsat MSS 2	12 March 1975	LM21860611975071AAA03	GloVis
Landsat TM	4 December 1984	LM51730611984339AAA03	GloVis
	19 July 1986	LT51730611986200XXX01	GloVis
	7 August 1987	LT51730611987219XXX05	GloVis
	4 August 1989	LT41730611989216XXX06	GloVis
	17 January 1995	LT51730611995001AAA01	GloVis
	2 February 1995	LT5173061009503310	GloVis
Landsat ETM+	6 December 1999	LE71730611999340SGS00	GloVis
	15 June 2000	LE71730612000167EDC00	GloVis
	3 September 2000	LE71730612000247EDC00	GloVis
	11 December 2001	LE71730612001345SGS00	GloVis
	31 January 2003	LE71730612003207EDC01	GloVis
	21 February 2005	LE71730612005052ASN00	GloVis
	15 January 2009	LE71730612009015ASN00	GloVis
	28 September 2009	LE71730612009271ASN00	GloVis
	18 January 2010	LE71730612010018ASN00	GloVis
Hyperion	28 May 2010	EO1H1730612010148110KF	GloVis
ALI	3 January 2012	EO1A1730612012003110PF	GloVis

captured the 1986 Nyamuragira flow as it was being emplaced, saturating the SWIR bands, and preventing the application of automated classification methods. The next best (cloud-free) Landsat image was acquired in 1987 and provided a clear image on which to apply the automated techniques, resulting in a robust classification. By choosing Landsat scenes as close to the eruption date as possible, we also increased the possibility of mapping lava flows prior to the emplacement of subsequent, overlapping flows.

All of the scenes were reprojected to the 15 June 2000 image using a UTM zone 35 south projection and the WGS 84 datum. Only bands 1–5 and 7 from the Landsat TM and ETM+ scenes were used, whereas bands 41–76 with 0.76–0.90 μm wavelengths from the hyperspectral Hyperion scene were used. These Hyperion wavelengths correspond to a single Landsat band (band 4), providing much higher spectral resolution than the single Landsat band. This band (4) was found to be most responsive to lava flow weathering and vegetation with age (Abrams *et al.* 1991). ALI and Landsat VSWIR bands cover a similar spectral range, although ALI data include three additional bands, providing a better spectral resolution than Landsat (table 1). All nine ALI VSWIR bands (1–7), therefore, were used to map the 2011 flow. The thermal infrared (TIR) band did not prove to be crucial for our mapping; thus, excluding this band from the Landsat datasets provided a fixed spatial resolution for all bands. The Landsat MSS scene was resampled to 30 m in order to allow a direct comparison with the TM/ETM+ imagery.

2.2. *Principal components analysis (PCA)*

Principal components analysis (PCA) on both TIR and VSWIR satellite data has been successfully used to map lava flows and volcanic tephra units for individual and

multiple flows (e.g. Abrams *et al.* 1991, 1996; Legeley-Padovani *et al.* 1997; Wiart *et al.* 2000). A PCA was performed on the Landsat and ALI datasets, but not on the Hyperion image as the latter included only 0.76–0.90 μm wavelengths. The Landsat and ALI images were subset around the lava flow field to permit a faster analysis because fewer pixels were input into the PCA.

For each multi-spectral satellite image, several bands may contain similar information. The purpose of a PCA is to reduce this redundancy by comparing the spectral information in each band with that in every other band via an orthogonal transformation, so that the first principal component (PC) represents the greatest variance of the data, the second PC represents the second greatest variance of the data, and so on. The number of PCs generated is equivalent to the number of input bands; for example, six PCs were generated for the Landsat TM and ETM+ data. Since the PCA technique compresses the useful spectral information into fewer, uncorrelated components, the scene can be represented by $\sim$3 components rather than six bands and overall noise is reduced.

2.3. *PCA evaluation*

Prior to attempting a classification of the flows, three PCs were chosen that best highlighted the flow of interest (figure 2). For roughly half of the lava flows, the first three PCs provided the best contrast between the lava flow and the surroundings and were, therefore, combined for subsequent unsupervised classification. We only deviated from using PCs 1–3 when other PCs more clearly highlighted the flow of interest (e.g. 1981, 1984 and 2001, as well as parts of the 1996 and 2000 flows). To investigate why deviations from PCs 1–3 were necessary, we examined our factor loading calculations (Appendix A) for each of the Landsat scenes we used. The factor loadings are coefficients of the PCA transformation and determine which bands of the original imagery contributed most to each PC.

Regardless of whether we used PCs 1–3 or deviated from this combination, the most dominate contributions to the PCs used were from bands 1, 2, 3 and, less extensively, band 4 of the original data. This appears to correlate with the large amount of vegetation in each Landsat scene. Band 1 is responsive to waterbodies and blue chlorophyll absorption in vegetation, band 2 is responsive to blue and red chlorophyll absorption and green reflectance of healthy vegetation, band 3 is responsive to red chlorophyll absorption of healthy vegetation, and band 4 is sensitive to the amount of vegetation biomass in the scene. In only two instances did band 5 contribute to a PC used (Appendix A) – for the 1996 and 2000 flows we used PCs 1, 2 and 4. PCs 1 and 2 comprised reflectance from bands 1, 2, 3 and 4, while PC 4 comprised reflectance from bands 1, 3 and 5. Band 5 is sensitive to turgidity (water) in plants. This Landsat scene was acquired in September, which is within one of the two annual rainy seasons in the Virunga (http://www.eoearth.org/article/Virunga_-National_Park,_Democratic_Republic_of_Congo#gen7); therefore, the response in band 5 probably results from moisture-rich vegetation. As most of the reflectance in each scene results from the abundant vegetation in the area, the flows of interest were easily identifiable due to the stark contrast between vegetation and barren lava.

The user determines the number of classes to be generated within the classification program. Since our input into the classification program are three PCs, and PCA is an orthogonal transformation of the original data, the classification program creates each class based on the distribution of the data along the entire length of the first PC

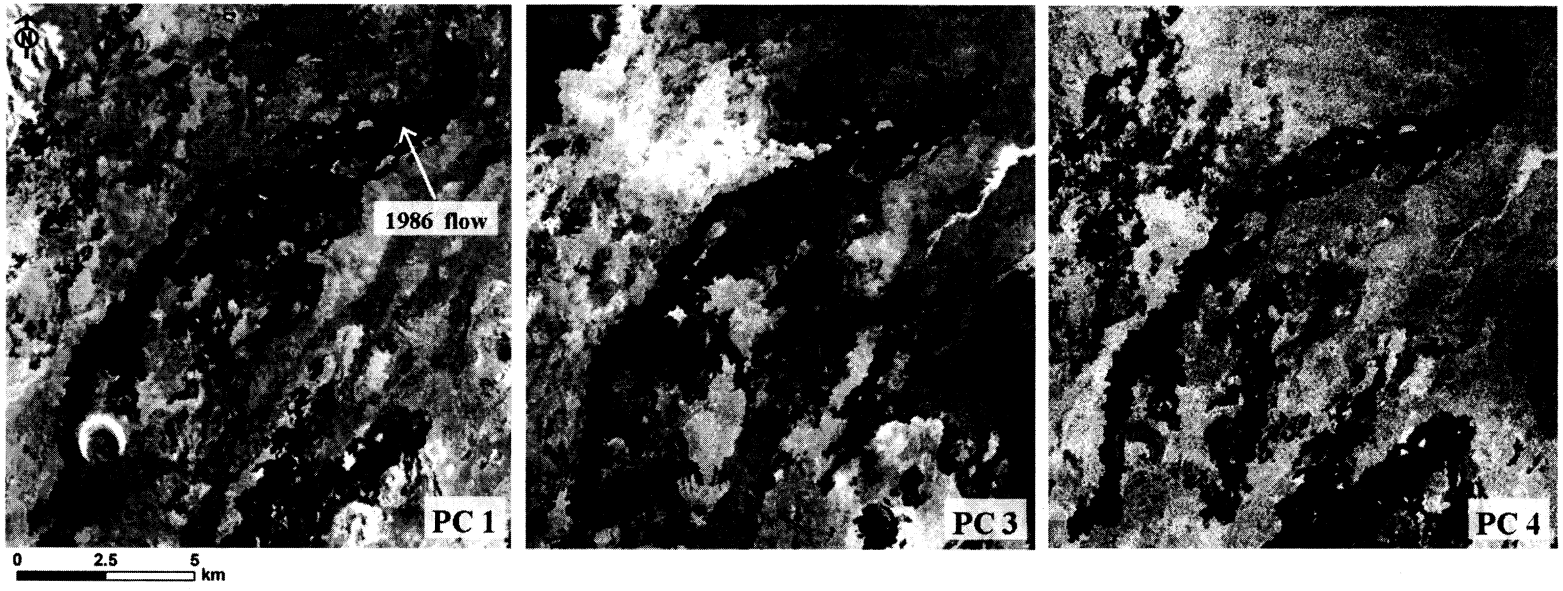

Figure 2. Images showing the three principal components (PCs; 1(*a*), 3(*b*), 4(*c*)) input into the unsupervised classification module (ISODATA) to map the 1986 Nyamuragira lava flow. These three PCs best discriminated the flow from the rest of the scene.

axis. Because the first PC contains the greatest variance of data, there is an increased separation of reflectance between, for example, bare rock/soil and vegetation along this axis compared to the raw data (see Jensen (2007) for more detail). This separation appears to result from the contrast between recent lava flows, which have lower reflectance, and older lava flows and forest, which have greater reflectance due to weathering and (re)vegetation. A qualitative assessment of this separation is shown in figure 2. The 1986 lava flow is noticeably darker than its surroundings in PC1 and PC4, indicating a clear spectral separation. Colour-composites of the original Landsat image (figure 3 (*a*)) and the combined 3-PC image (figure 3 (*b*)) are shown to illustrate that the PCA allows a more clear separation of lava flow and surrounding vegetation. This may not always be apparent in the original imagery and, therefore, transformations of this kind are valuable.

2.4. *Unsupervised classification*

The three PCA images chosen were cropped to include the area just around the flow being mapped, which again permitted a faster, more accurate classification because fewer pixels had to be evaluated and grouped into classes. Since a PCA was not performed on the Hyperion scene, the original image was cropped to include the areas just around the 2010 flow and an unsupervised classification was carried out on the original data. Relative locations and extents of the flows were determined based on the Smithsonian's GVN reports (Smithsonian Institution 1971–2011) and verified by observing two scenes bracketing the flow's emplacement. As discussed above, an unsupervised classification (also known as ISODATA; see Jensen (2007) for more detail) is carried out using digital image processing software such as ERDAS Imagine (Appendix B). The unsupervised classification program compares the

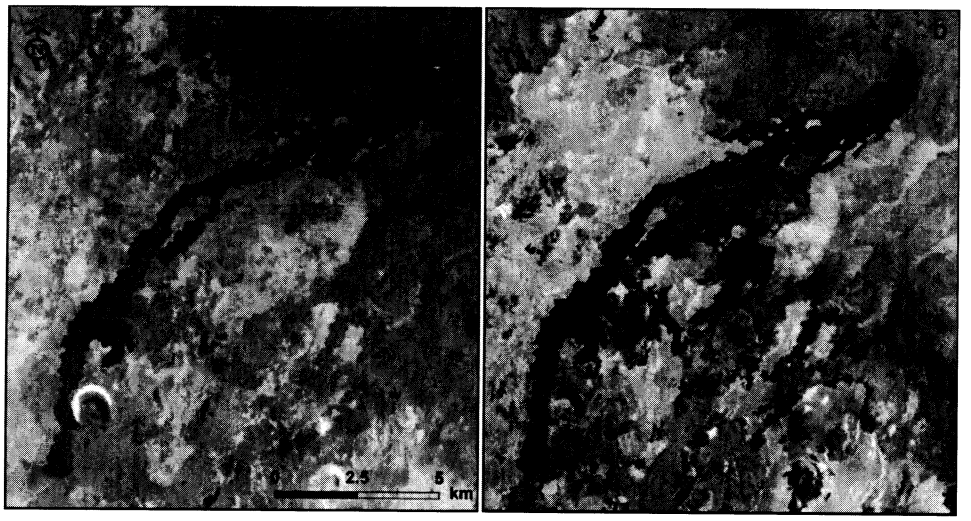

Figure 3. Colour-composite images of (*a*) the original Landsat data (acquired 7 August 1987) with bands 4, 3 and 2 displayed in red, green, and blue, and (*b*) the three PCs (1, 3, 4) displayed in red, green, and blue. The 1986 Nyamuragira lava flow is more easily distinguished, both visually and spectrally, in the PC image compared to the original image.

reflectance of each pixel to every other pixel in the scene and groups similar reflectances into classes.

A supervised classification was also attempted to determine if this might produce a more accurate lava flow map. In this type of classification, training sets are acquired for each land feature (lava flow, vegetation, water, cities) and then input into the classification program. Compared to our unsupervised classification results, the supervised classification method did not produce a more accurate lava flow map. Acquisition of training sets is time-consuming and, although the results of this method are similar to the unsupervised classification, we found the latter to be the most efficient method.

We choose the 1986 and the 2004 Nyamuragira lava flows to demonstrate our methodology, as the former was one of the more apparent flows to map and the latter illustrates the limitations of the methods we used. The entire 1986 flow was erupted onto considerably older and more weathered flows (1938–1940, 1948 and 1976–77), providing ample spectral contrast with its surroundings (figures 3 and 4 (*a*)). The 2004 lava flow, on the other hand, was more difficult to map using this method. Near the summit area, spectral contrast between the 1998, 2001, 2002 and 2004 lava flows was very low (figure 4 (*d*)). This inhibited both visual separation of the 2001, 2002 and 2004 flow boundaries and the ability of the unsupervised classification to classify the separate flows. Further down the flanks, the spectral contrast increases, allowing a clearer visual separation, as well as automated classification.

2.5. *Mapping the delineated lava flows*

After the unsupervised classification, we found that some of the lava flows were defined by one class (1971, 1984, 1986 and 1991), while the remaining flows were defined by more than one class. The latter was due to spectral variation within the flow, potentially caused by early revegetation of parts of the flow (if the imagery used to map the flow was acquired over $\sim$5 years after flow emplacement) or by intra-flow features such as varied lava textures (e.g. Spinetti *et al.* 2009) resulting from slope changes. We also found that, in some instances, the lava flow and parts of the surroundings were included in the same class (e.g. figure 4 (*a*) – yellow spots surrounding the 1986 flow, which is also displayed in yellow). Using a module in ERDAS Imagine ("clump"), we were able to reassign the surrounding spots to a different class number and separate these from the main flow (figure 4 (*b*)). At this point, the class or classes that were identified as the flow were reassigned a value of one and the remaining classes were assigned a value of zero (figure 4 (*c*)). Creating this binary image was necessary to clearly delineate the flow from the surrounding non-flow features. The area of each flow was determined by multiplying the pixel count of the flow by the pixel area (table 1).

In the absence of recent field-based lava flow thickness measurements, we used a previously reported value to determine a volume for each lava flow. Kasahara *et al.* (1991) determined that an average thickness of 3 m was most appropriate based on compiled research of past Nyamuragira eruptions and, therefore, we also adopt this value. We considered DEM subtraction to better constrain this value, but the vertical resolution of available DEMs is too coarse to improve upon the thickness estimate of Kasahara *et al.* (1991) via DEM subtraction. The 3-m thickness of Nyamuragira's flows is significantly less than the average 5–16 m vertical accuracy of

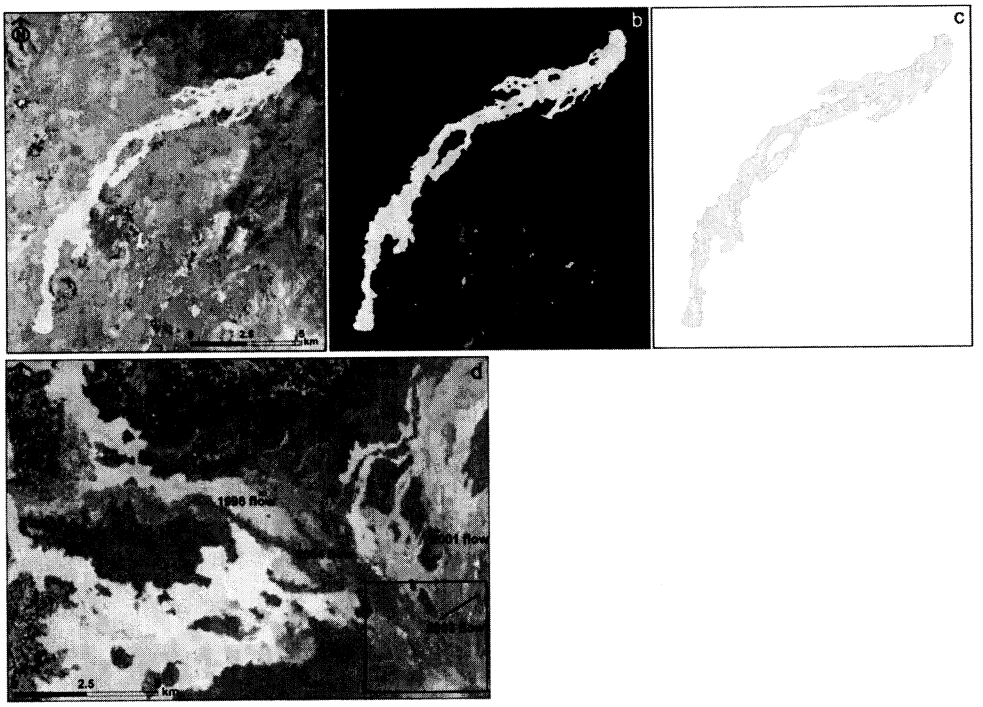

Figure 4. (*a*) Results of the unsupervised classification of the 7 August 1987 Landsat scene, showing the 1986 flow highlighted in yellow. Yellow patches around the 1986 flow were falsely classified; (*b*) The false pixels were easily reassigned as "non-flow" using a module in ERDAS Imagine (clump); (*c*) The final result, a binary image, is produced by reassigning the background classes as "0" and the lava flow as "1", which allowed a clear separation of the 1986 flow; (*d*) Results of an unsupervised classification of the 21 February 2005 Landsat scene. The 2004 was more difficult to map as the overlapping flows emplaced with ~1 year of each other had very similar spectral signatures (see black box). However, note how the flows become easier to separate (spectral signatures are different from surroundings) down the volcano flanks.

DEMs created from satellite imagery such as ASTER (7–15 m; Hirano *et al.* 2003), SPOT (~5 m; Endreny *et al.* 2000) or SRTM (~16; Rodriguez *et al.* 2005) data. IKONOS-derived digital surface models (DSMs) have a vertical accuracy of 2–5 m, although the lower estimate was a result of flat terrain, and for vegetated surfaces, like Nyamuragira, this value increases (Poon and Fraser 2005). DEMs derived from light detection and ranging (LiDAR) data are more accurate (0.5 m; Liu *et al.* 2007), although LiDAR topographic data of the Virunga region are unavailable. Even if the political situation improves, acquisition of this type of data would be very costly due to the large spatial extent of the flows.

2.6. *Special case: MSS imagery*

Landsat MSS has fewer spectral bands than the TM and ETM+, requiring a different processing scheme for the 1975 MSS image prior to the unsupervised classification. The 1971 lava flow abutted a body of water. The available Landsat MSS bands detected similar spectral signatures for both water and lava, rendering

them indistinguishable through the unsupervised classification. Masking the water from the stacked PC image remedied the effect and an unsupervised classification was successfully performed on the 1975 image.

3. Lava flow map and derived volumes

3.1. *Comparison of our lava volumes with previous studies*

The map of Nyamuragira lava flows produced from the Landsat, Hyperion and ALI image analysis is shown in figure 5. Table 3 shows lava flow volumes calculated using the technique described above, and a comparison of our results with previously reported lava volumes (Kasahara *et al.* 1991; Smets *et al.* 2010; Colclough 2005). Nyamuragira eruptions from 1967 to 2011 produced between 0.005 and 0.136 km^3 of lava per eruption. While our data generally agree with the volumes reported by Kasahara *et al.* (1991) for the eight eruptions between 1967 and 1991, there are some differences (table 3). Colclough (2005) estimated minimum lava flow volumes for the 1998 (71×10^6 m^3) and 2001 (133×10^6 m^3) Nyamuragira eruptions; our estimates agree well with their results for the 2001 flow and are within 20% of their results for the 1998 flow. In a comparison with Smets *et al.* (2010), our estimates agree to within 10% of theirs, except for the 1998 flow (17% difference).

On 31 May 2003, Landsat ETM+ lost its scan line corrector (SLC) and, as a result, stripes of missing data appear in the image. The imagery used to map the 2006 flow was affected by this condition. We were able to map the 2006 flow with the same methods used to map the older flows, although this scene did require some digitization in ArcGIS after the binary image from the classification was complete, particularly in the area covered by clouds. The flow was delineated with the aid of a Landsat ETM+ scene acquired on 28 September 2009, as well as an ASTER image acquired on 31 August 2007. Eight out of the 19 flows (1976, 1980, 1991, 1989, 2000, 2001, 2003 and 2004) required small amounts of digitization after the classification to remove falsely classified flow surroundings, which were not possible to separate using the digital image processing software. Four out of these eight instances were associated with the overlapping flows near the summit area. Due to either atmospheric or eruption clouds obstructing parts of the 1967, 1996, 2000, 2006, 2010 and 2011 flows, these also required small amounts of digitization. The remaining five flows (1971, 1981, 1984, 1986 and 1994) were mapped with no post-processing.

4. Discussion

4.1. *Temporal changes in lava flow spectral signature*

From our PC analyses, we conclude that most of the spectral variation within the Landsat and ALI scenes is due to vegetation and water reflectance, and that the comparatively low reflectance of the lava flows (bare rock) provides high contrast with the surrounding vegetation that allows the flows to be easily mapped with unsupervised classification methods. If a new lava flow is emplaced on older but relatively recent lava, the efficacy of the technique depends on the vegetation and weathering rate of the flows. Ground, aerial and satellite studies of basaltic flow

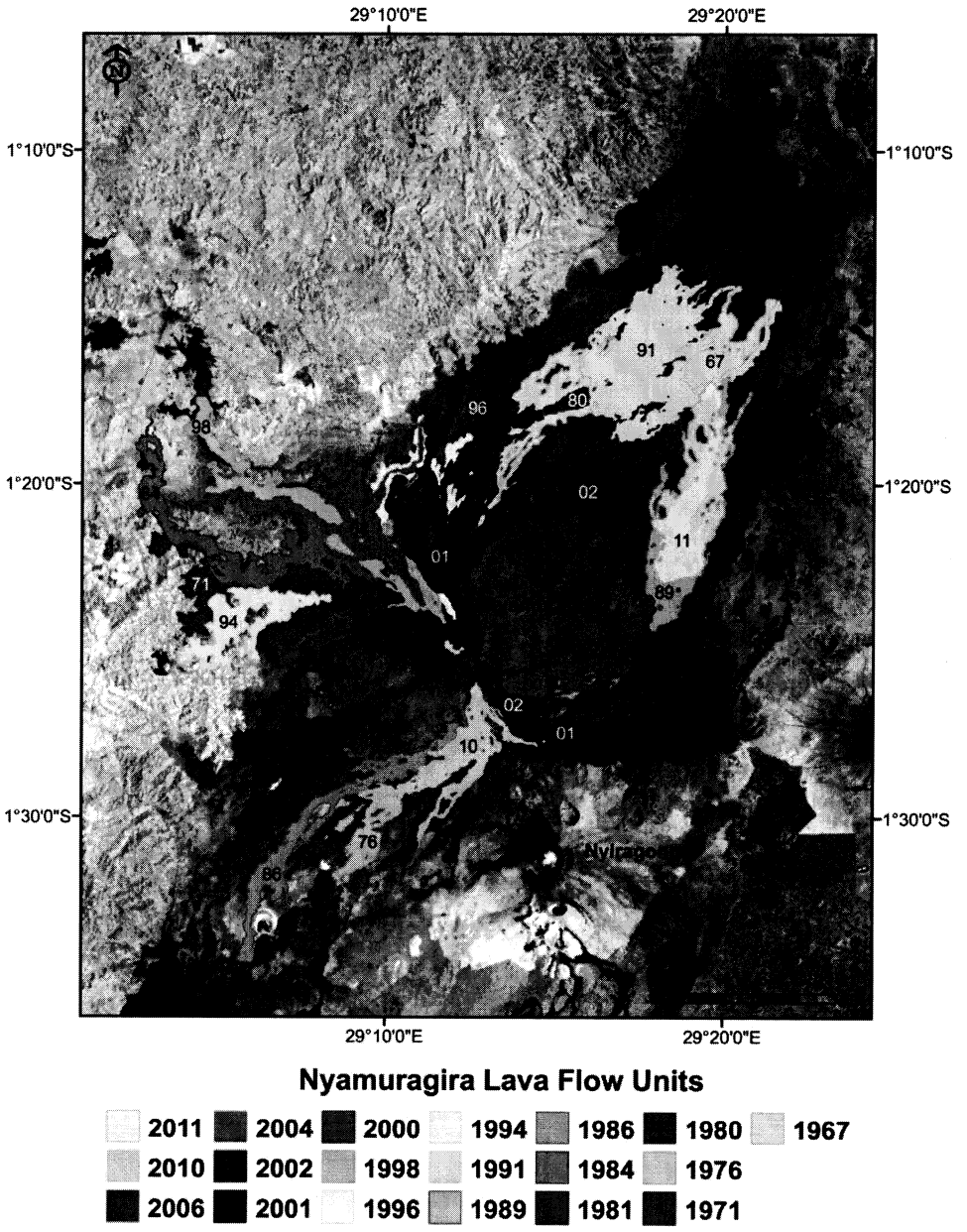

Figure 5. Map of Nyamuragira lava flows erupted from 1967 to 2011. The base map is a Landsat ETM+ scene acquired on 21 February 2005 (band 4).

fields have shown that changes in VSWIR (0.4–2.4 μm) spectral signatures result from electronic transitions in iron in various oxidation states, as well as the increasing extent of vegetation, as weathering progresses (Bonneville *et al.* 1988; Abrams *et al.* 1991; Kahle *et al.* 1995; Spinetti *et al.* 2009). In order to assess how individual flows change through time with respect to vegetation and weathering, we must look at the reflectance of each lava flow, instead of the reflectance from the

Table 3. A comparison between Nyamuragira lava volumes we derived (1967–2011) and those of other more recent studies. Smets *et al.* (2010) did not derive lava volumes for 1967–1976 flows, but instead used volumes cited in Burt *et al.* (1994), which were originally cited in Kasahara *et al.* (1991).

				Volume (10^6 m^3)			
Start	End	Eruption duration (days)	Repose (prior to eruption; days)	Kasahara *et al.* (1991)	Colclough *et al.* (2005)	Smets *et al.* (2010)	this study
23 April 1967	3 May 1967	11	3076	95	–	–	92
24 March 1971	Mid-May 1971	~53	1415	90	–	–	70
23 December 1976	April 1976	~267	2050	62	–	–	50
30 January 1980	23 February 1980	25	959	87	–	67	63
25 December 1981	14 January 1982	20	671	124	–	126	122
23 February 1984	14 March 1984	21	770	84	–	68	66
16 July 1986	20 August 1986	36	854	72	–	55	63
30 December 1987	3 January 1988	5	497	5	–	6	5
24 April 1989	August 1989	~114	477	114	–	95	90
20 September 1991	8 February 1993	508	766	100	–	131	128
4 July 1994	25 August 1994	53	511	–	–	43	36
1 December 1996	17 December 1996*	16	829	–	–	50	52
17 October 1998	31 October 1998*	14	669	–	71	69	57
27 January2000	17 February 2000*	21	453	–	–	47	46
6 February 2001	5 April 2001	59	355	–	133	140	137
25 July 2002	2 September 2002	40	476	–	–	57	63
8 May 2004	14 June 2004	37	614	–	–	69	73
27 November 2006	5 December 2006	9	896	–	–	44	46
2 January 2010	27 January 2010	26	1124	–	–	53	49
6 November 2011	–	–	651	–	–	–	71

*Eruption end dates derived from TOMS SO_2 measurements.

entire scene. To do this, we used statistics from one of the Landsat scenes, which provided quantitative information about the weathering and vegetation processes that occur on these flows over time. The purpose of this exercise is to determine how quickly Nyamuragira flows vegetate and to investigate if a new flow, erupted over an older flow, can be distinguished spectrally from the older flow.

To determine quantitatively how lava flow spectral reflectance changes over time, we used the Landsat ETM+ scene acquired on 21 February 2005 as this scene provides a cloud-free view of all but the 2006, 2010 and 2011 flows. We corrected this image for atmospheric and radiometric effects using the COST model (Chavez 1996) but performed no PCA or unsupervised classification on the image in order to conserve the characteristics of the original data. The advantages of using a single image are that vegetation, sun angle and atmospheric conditions are constant. Otherwise, if two images acquired on different days are compared, parameters such as seasonal differences in vegetation may affect the spectral signatures and not allow a direct evaluation. We measured the reflectance spectrum of each Nyamuragira lava flow at several locations along the flow and averaged the values. This allowed us to compare reflectance spectra and determine how the reflectance changes with age. A terminal lobe of the 1958 Nyamuragira lava flow was also transected to obtain an older end member. Only the terminus of the 1958 flow was exposed in the 2005 image and, therefore, a near-vent sample could not be acquired. In fact, several flows within this image were overlapped by more recent flows and did not provide a full vent-to-terminus sampling. In these situations, as many measurements as possible were taken within the exposed area. We obtained an average band-4 reflectance of the 2010 flow (0.05) from the Hyperion scene and a spectral profile of the 2011 flow (band 4=0.01) from the ALI scene. These values are lower than 1967–2005 band-4 reflectances shown in figure 6. Spectral profiles were also sampled for vegetated areas around the flows and these reflectances were the highest of all sampled ($\sim$0.7).

Spectral variations in the visible portion of the spectrum (bands 1–3) are typically associated with changes in the oxidation state of iron in lava flows as the flows age (Abrams *et al.* 1991). We do not see any systematic change in the reflectivity of bands 1–3 with age. Instead, we found the largest variation in spectral reflectance in ETM+ band 4 and so we focus on the interpretation of this band (figure 6). Reflectance in band 4 clearly increases with flow age, which we assume is in part due to vegetation growth (biomass) and the spectral "red-edge"; the rapid increase in the reflectance of vegetation at near-IR wavelengths (Abrams *et al.* 1991; Filella and Penuelas 1994; Seager *et al.* 2005). A general increase in band-4 reflectivity with lava flow age was also found in a multi-parameter study of nine alkaline Etnean lavas (1607–2003), in which field data and lava flow spectral signatures from a ground-based spectro-radiometer and hyperspectral satellite data were compared (Spinetti *et al.* 2009). They found that vegetation growth and weathering with time were responsible for the increase, while tephra cover (differences in grain size) decreased a lava flow's reflectivity. During a field campaign in 2006, we noted that tephra was mainly found only near-vent at the 1986 and 2006 Nyamuragira eruption vents. If this is true for the rest of the vents, this suggests that tephra does not have a strong influence on the spectral signatures along the length of the flow.

Using SAR, Rodriguez *et al.* (2001) found that Nyamuragira lava flows vegetate completely within $\sim$30 years. In lava flows under 30 years old, they found a positive correlation between the SAR signal and soil formation (weathering)/vegetation of Nyamuragira flows. We investigated how vegetation changes over time at

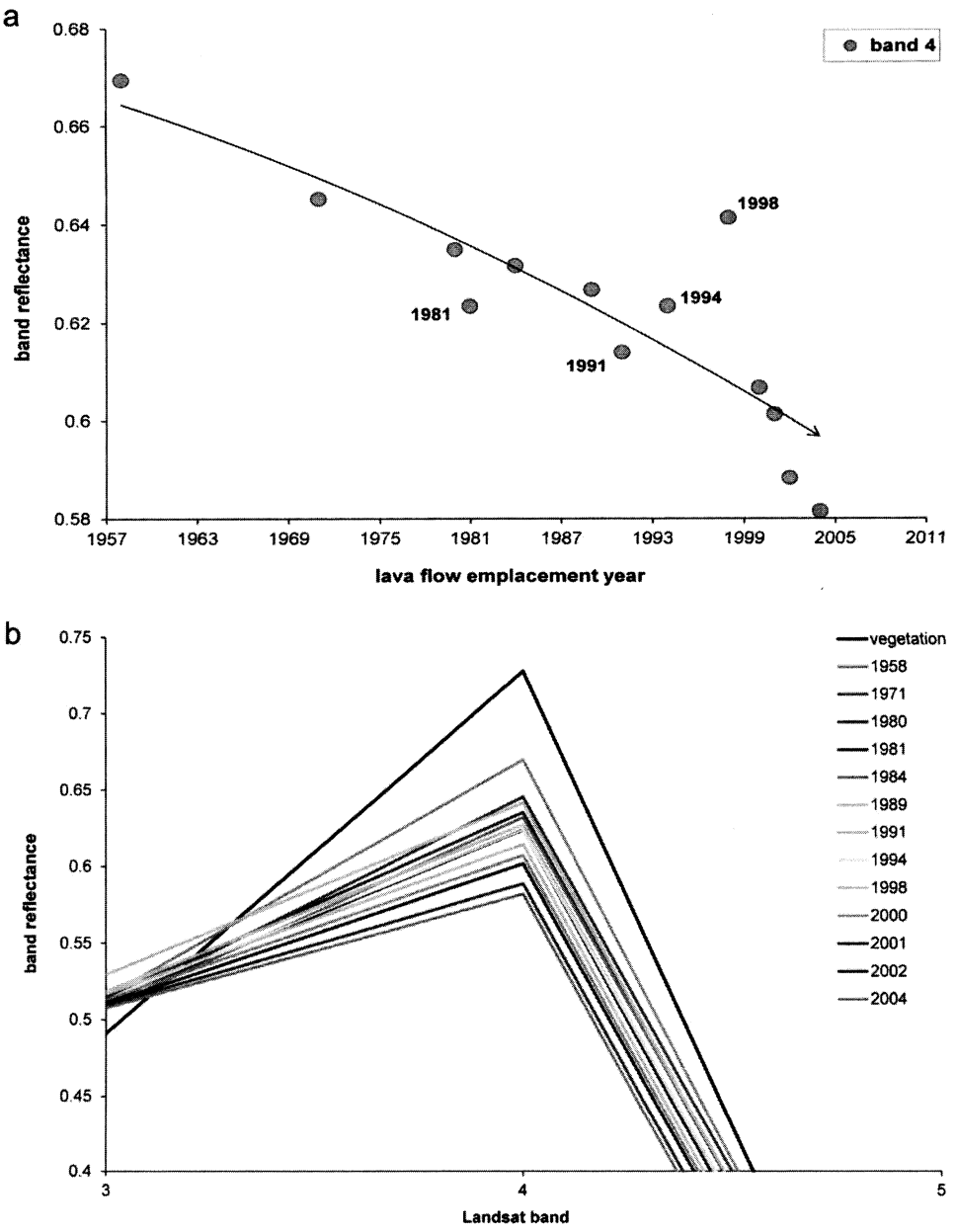

Figure 6. (*a*) Spectral profiles from transects of Nyamuragira lava flows (1958–2005) from vent to terminus (when possible) are averaged as single points for each flow year. A clear increase in band 4 reflectance indicates revegetation of the flows as they age. The Landsat ETM+ scene used for these transects was acquired on 21 February 2005, hence the lack of the 2006, 2010, and 2011 data points. Band-4 reflectances of the 2010 and 2011 lava flows from Hyperion and ALI imagery, respectively, are lower than 1958–2005 values. (*b*) A graphical presentation of the above points illustrates the flows that deviate from the progression.

Nyamuragira by utilizing the normalized difference vegetation index (NDVI: band 4-band 3/band 4+band 3), which determines the amount of green vegetation in a scene. The result is an image in which pure black represents no healthy vegetation

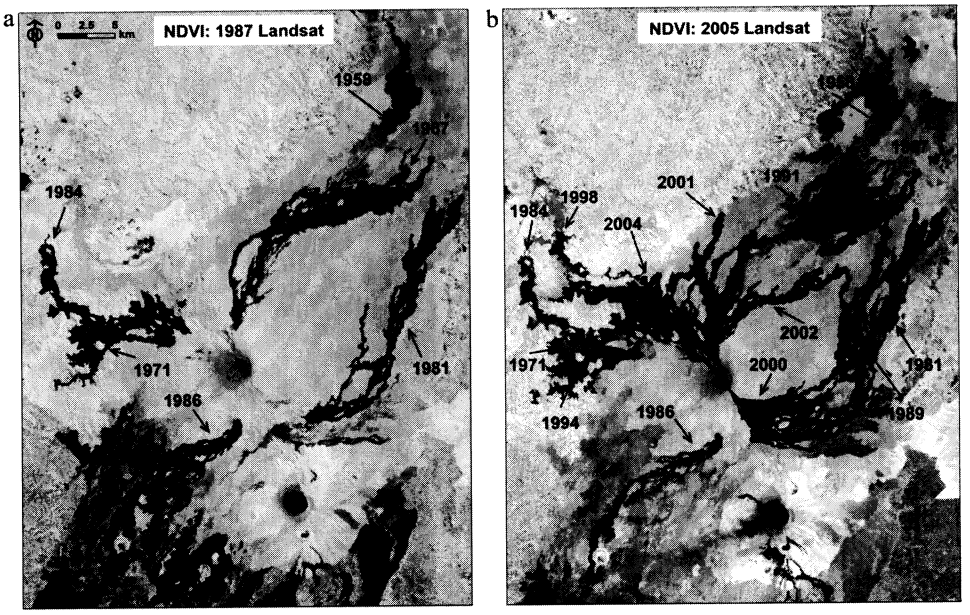

Figure 7. Normalized difference vegetation index (NDVI) results for the Landsat TM scene acquired on 7 August 1987 and the Landsat ETM+ scene acquired on 21 February 2005. The scale is 0–1; 0 is displayed as pure black and indicates no vegetation, where 1 is displayed as pure white and indicates complete vegetation. Revegetation of Nyamuragira lava flows results in significant NDVI increases, where lava flows ~5 years apart can be distinguished spectrally (and/or visually) from one another.

and pure white represents complete healthy vegetation cover (figure 7). We find that the NDVI values increase with increasing lava flow age and indicate revegetation within ~5 years of lava flow emplacement. Vegetation, and to some degree weathering, therefore, provides the best explanation for our results. Exceptions include the 1998 flow (on the western flank), which has a higher reflectance than expected for its age and the 1991 flow (on the northern flank), which has a lower reflectance than expected. The flows that deviate from the overall band-4 increase could have weathered and/or vegetated differently than surrounding flows. Future ground-based investigations would be helpful to resolve these differences. Based on the spectral profiles and NDVI results, it appears that most flows will start to revegetate and weather sufficiently within ~5 years in order for band-4 reflectances and NDVI values to differ markedly from a fresh flow. This contrast greatly facilitates the mapping of lava flows emplaced through heavily vegetated areas (forest) and on top of previously erupted flows (older flows which are in the process of revegetating) in the Virunga region.

4.2. *Lava flow volume errors*

We identify three sources of potential error within our volume estimates using Landsat, Hyperion, and ALI data: (1) inaccurate lava flow boundaries due to the flow edge occupying only part of a Landsat/Hyperion/ALI pixel; (2) erroneous inclusion of surrounding substrate as lava flow and (3) the average lava flow

thickness used. Even in the most extreme case (an off-set of one pixel for the entire perimeter of the largest lava flow, 2001), the perimeter of the flow only accounts for $\sim 16\%$ of the total flow area. In reality, these errors would be negligible as some perimeter pixels will be within and others outside of the chosen boundary. The second error was greatest when overlapping flows near the summit were difficult to delineate (e.g. it would be a $\sim 20\%$ difference if we assumed that the 2004 flow in figure 4 (*d*) extended to the summit, compared to its actual extent, seen in figure 5). However, the largest source of error, as Smets *et al.* (2010) also points out, was the flow thickness. Calculating volumes with a 1 and 5 m thickness (3 ± 2 m) results in a 200–400% difference in the largest flow volume (2001) compared to the volume calculated with the average 3 m thickness. Since Smets *et al.* (2010) and Colclough (2005) also use the 3 m average lava thickness suggested by Kasahara *et al.* (1991), our volume estimate comparisons are actually comparisons of lava flow areas. The good agreement between our data and these prior estimates suggest that we have similarly detected flow boundaries.

5. Conclusions

Mapping Nyamuragira's lava flows using PCA and automated unsupervised classification techniques has proven successful for most eruptions of the volcano since 1967. Unsupervised classification resulted in well-separated classes, which allowed easy discrimination of lava flows from surrounding features. The spectral contrast between flows that permits accurate mapping reflects (re)vegetation and weathering of the flows with time; revegetation progresses enough within ~ 5 years that the reflectance and NDVI values are significantly different than those of younger flows.

Overlapping lava flows emplaced within small time spans (e.g. the 2000 and 2001 flows to the SE or the 1998, 2002 and 2004 flows to the NW) required post-processing to delineate boundaries nearest the summit. This was accomplished through examination of images acquired prior to and after the emplacement of the flow in question to discern some of the overlapping boundaries. Experimenting with band combinations during the process allowed overlapping flows to be more easily separated. During this post-processing, more difficulty occurred when delineating flows closer to the summit crater, possibly due to the larger extent of overlapping flows, slope effects (e.g. thinner flows being more easily weathered) or satellite geometry.

We found that the use of automated classification methods with VSWIR satellite imagery for mapping lava flows is useful and cost-effective in regions such as Virunga, particularly for lava flows erupted through vegetation or emplaced on top of older, revegetating lava flows (>5 years). In these situations, where cloud-free satellite imagery is available, this method is faster than manually digitising flow perimeter, especially for flows with intricate flow paths around elevated areas called kipukas. Even in situations where some digitization is needed after the automated classification routine due to cloud cover or spectral ambiguity, the automated methods can serve as an aid to mapping by performing the initial work more quickly. In the case of digitization alone (no automated methods), the time required to map a flow varies greatly and depends on the size of the flow, the dataset being used (e.g. resolution), and the level of flow complexity the user wants to display. With automated methods, on the other hand, the size of the flow does not significantly

increase the processing time. Furthermore, the automated techniques and PCA provide insights into the underlying subtle spectral differences between the lava flows, whereas manual techniques do not.

In situations where overlapping flows are present, the automated method could be used with radar, which has proven useful for separating the flows based on roughness differences. In addition, the ability of radar to penetrate clouds is advantageous in this equatorial area due to the cloud cover that often obscures optical satellite imagery. However, VSWIR imagery is still often needed in conjunction with radar to delineate boundaries (e.g. Colclough 2005; Smets *et al.* 2010). Our derived lava flow volumes for Nyamuragira eruptions from 1967 to 2010 are similar to those previously reported lava volumes (Kasahara *et al.* 1991; Colclough 2005; Smets *et al.* 2010). At the time of writing, this is the first estimated lava volume for the 2011 flow. Although lava flow overlap occurred more in flows emplaced between 1994 and 2010 due to a concentration of activity in a NW-SE rift zone since 1996, the percentage of overlap was small compared to the entire area of the flow.

Acknowledgements

Funding for this work was provided by the US National Science Foundation (grant EAR 0910795 to SAC). We would like to thank Scott Rowland for his thorough review of an earlier version of the manuscript, and two anonymous reviewers for their constructive comments, all of which greatly improved the manuscript.

References

Abrams, M., Abbott E. and Kahle, A., 1991, Combined use of visible, reflected infrared, and thermal infrared images for mapping Hawaiian lava flows. *Journal of Geophysical Research*, **96**, pp. 475–484.

Abrams, M., Bianchi, R. and Pieri, D., 1996, Revised mapping of lava flows on Mount Etna, Sicily. *Photogrammetric Engineering and Remote Sensing*, **62**, pp. 1353–1359.

Aoki, K., Yoshida, T., Yusa, K. and Nakamura, Y., 1985, Petrology and geochemistry of the Nyamuragira Volcano, Zaire. *Journal of Volcanology and Geothermal Research*, **25**, pp. 1–28.

Bluth, G.J.S. and Carn, S.A., 2008, Exceptional sulfur degassing from Nyamuragira volcano, 1979–2005. *International Journal of Remote Sensing*, **29**, pp. 6667–6685.

Bonneville, A., Lanquette, A.M., Pejoux, R. and Bayon, C., 1988, Reconnaissance des principales unites geologiques du Piton de la Fournaise, La Reunion, a partir de SPOT1. *Bulletin de la Societe geologique de France*, **8**, pp. 1101–1110.

Burt, M.L., Wadge, G. and Scott, W.A., 1994, Simple stochastic modeling of the eruption history of a basaltic volcano: Nyamuragira, Zaire. *Bulletin of Volcanology*, **56**, pp. 87–97.

Carn, S.A., 1999, Application of synthetic aperture radar (SAR) imagery to volcano mapping in the humid tropics: A case study in East Java, Indonesia. *Bulletin of Volcanology*, **61**, pp. 92–105, doi: 10.1007/s004450050265.

Carn, S.A. and Oppenheimer, C., 2000, Remote monitoring of Indonesian volcanoes using satellite data from the Internet. *International Journal of Remote Sensing*, **21**, pp. 873–910, doi: 10.1080/014311600210344.

Carn, S. and Bluth, G.J.S., 2003, Prodigious sulfur dioxide emissions from Nyamuragira volcano (D.R. Congo). *Geophysical Research Letters*, **30**, pp. 2211, doi:10.1029/2003GL018465.

CARN, S., KRUEGER, A.J., BLUTH, G.J.S., SCHAEFER, S.J., KROTKOV, N.A., WATSON, I.M. and DATTA, S., 2003, Volcanic eruption detection by the Total Ozone Mapping Spectrometer (TOMS) instruments: A 22-year record of sulphur dioxide and ash emissions. In *Volcanic Degassing*, C. OPPENHEIMER, D.M. PYLE and J. BARCLAY (Eds.), pp. 177–202 (London: Geological Society, Special Pubs, 213).

CHAVEZ, P.S., 1996, Image-based atmospheric corrections-revisited and improved. *Photogrammetric Engineering and Remote Sensing*, **62**, pp. 1025–1036.

COLCLOUGH, S.J., 2005, Investigations of Nyamuragira and Nyiragongo volcanoes (DRC), Using interferometric synthetic aperture radar, PhD dissertation, University of Cambridge, UK.

CROWN, D.A. and BALOGA, S.M., 1999, Pahoehoe toe dimensions, morphology, and branching relationships at Mauna Ulu, Kilauea Volcano, Hawaii. *Bulletin of Volcanology*, **61**, pp. 288–305, doi:10.1007/s004450050298.

EBINGER, C. and FURMAN, T., 2002, Geodynamical setting of the Virunga volcanic province, East Africa. *Acta Vulcanologica*, **15**, pp. 9–16.

ENDRENY, T.A., WOOD, E.F. and LETTENMAIER, D.P., 2000, Satellite-derived digital elevation model accuracy: Hydogeomorphological analysis requirements. *Hydrological Processes*, **14**, pp. 1–20.

FILELLA, I. and PENUELAS, J., 1994, The red edge position and shape as indicators of plant chlorophyll content, biomass, and hydric status. *International Journal of Remote Sensing*, **15**, pp. 1459–1470.

HARRIS, A.J.L., WRIGHT, R. and FLYNN, L.P., 1999, Remote monitoring of Mount Erebus Volcano, Antarctica, using polar orbiters: Progress and prospects. *International Journal of Remote Sensing*, **20**, pp. 3051–3071.

HAYASHI, S., KASAHARA, M., TANAKA, K., HAMAGUCHI, H. and ZANA, N., 1992, Major element chemistry of recent eruptive products from Nyamuragira volcano, Africa (1976–1989). *Tectonophysics*, **209**, pp. 273–276.

HIRANO, A., WELCH, R. and LANG, H., 2003, Mapping from ASTER stereo image data: DEM validation and accuracy assessment. *ISPRS Journal of Photogrammetry and Remote Sensing*, **57**, pp. 356–370.

JENSEN, J.R., 2007, *Remote Sensing of the Environment: An Earth Resource Perspective*, 2nd Edition, pp. 608 (Upper Saddle River, NJ: Pearson Prentice Hall).

KAHLE, A.B., ABRAMS, M.J., ABBOTT, E.A., MOUGINIS-MARK, P.J. and REALMUTO, V.J., 1995, Remote sensing of Mauna Loa. In *Mauna Loa Revealed: Structure, Composition, History, and Hazards*, J.M. RHODES and J.P. LOCKWOOD (Eds.), pp. 145–170 (Washington, DC: American Geophysical Union, Geophysical Monograph, 92).

KAMPUNZU, A.B., BONHOMME, M.G. and KANIKA, M., 1998, Geochronology of volcanic rocks and evolution of the Cenozoic Western Branch of the East African rift system. *Journal of African Science*, **26**, pp. 441–461.

KASAHARA, M., TANAKA, K. and ZANA, N., 1991, A flank eruption of volcano Nyamuragira in 1991. *Journal of African Studies*, **39**, pp. 29–50.

LEGELEY-PADOVANI, A., MERING, C., GUILLANDE, R. and HUAMAN, D., 1997, Mapping of lava flows through SPOT images – an example of the Sabancaya volcano (Peru). *International Journal of Remote Sensing*, **18**, pp. 3111–3133.

LU, Z., RYKHUS, R., MASTERLARK, T. and DEAN, K.G., 2004, Mapping recent lava flows at Westdahl Volcano, Alaska, using radar and optical satellite imagery. *Remote Sensing of the Environment*, **91**, pp. 345–353.

LIU, X., ZHANG, Z., PETERSON, J. and CHANDRA, S., 2007, LiDAR-derived high quality ground control information and DEM for image orthorectification. *Geoinformatica*, **11**, pp. 37–53.

MACKAY, M.E. and MOUGINIS-MARK, P.J., 1997, The effect of varying acquisition parameters on the interpretation of SIR-C radar data: The Virunga volcanic chain. *Remote Sensing of Environment*, **59**, pp. 321–336.

PATRICK, M.R., DEHN, J., PAPP, K.R., LU, Z., DEAN, K., MOXEY, L., IZBEKOV, P. and GURITZ, R., 2003, The 1997 eruption of Okmok Volcano, Alaska: A synthesis of remotely sensed imagery. *Journal of Volcanology and Geothermal Research*, **127**, pp. 87–105.

POON, J. and FRASER, C.S., 2005, Quality assessment of digital surface models generated from IKONOS imagery. *The Photogrammetric Record*, **20**, pp. 162–171.

RAY, R.G., 1960, *Aerial Photographs in Geologic Interpretation and Mapping*, Geological Survey Professional Paper 373, pp. 230 (Washington: U.S. Government Print Office).

RODRIGUEZ, K.M., WEISSEL, J.K. and MENKE, W.H., 2001, Lava-flow textural trends using SAR: The Virunga Volcanic Chain, East Africa. *Institute of Electrical and Electronics Engineers*, **5**, pp. 2421–2423, doi:10.1109/IGARSS.2001.978022.

RODRIGUEZ, E., MORRIS, C.S., BELZ, J.E., CHAPIN, E.C., MARTIN, J.M., DAFFER, W., HENSLEY, S., 2005, *An assessment of the SRTM topographic products, Technical Report JPL*, D-31639 (Jet Propulsion Laboratory, Pasadena, California).

ROWLAND, S.K., HARRIS, A.J.L., WOOSTER, M.J., AMELUNG, F., GARBEIL, H., WILSON, L., MOUGINIS-MARK, P.J., 2003, Volumetric characteristics of lava flows from interferometric radar and multispectral satellite data: The 1995 Fernandina and 1998 Cerro Azul eruptions in the western Galapagos. *Bulletin of Volcanology*, **65**, pp. 311–330.

SEAGER, S., TURNER, E.L., SCHAFER, J. and FORD, E.B., 2005, Vegetation's red edge: A possible spectroscopic biosignature of extraterrestrial plants. *Astrobiology*, **5**, pp. 372–390.

SELF, S., THORDARSON, T. and KESZTHELYI, L., 1997, Emplacement of continental flood basalt lava flows. In *Large Igneous Provinces: Continental, Oceanic, and Planetary Flood Volcanism*, J.J. MAHONEY, M.F. COFFIN (Eds.), pp. 381–410 (Washington, DC: American Geophysical Union, Geophysical Monograph, 100).

SHAW, H.R. and SWANSON D.A., 1970, Eruption and flow rates of flood basalts. In *Proceedings, Second Columbia River Basalt Symposium*, E.H. GILMOUR, D. STRADLING (Eds.), pp. 271–299 (Cheney: Eastern Washington State College Press).

SMETS, B., WAUTHIER, C. and D'OREYE, N., 2010, A new map of the lava flow field of Nyamuragira (D.R. Congo) from satellite imagery. *Journal of African Earth Sciences*, **58**, pp. 778–786.

SMITHSONIAN INSTITUTION, 1971–2011, Nyamuragira, Scientific Event Alert Network (SEAN) Bulletin, 7, No. 1 – Bulletin of the Global Volcanism Network, 37, No. 03.

SPINETTI, C., MAZZARINI, F., CASACCHIA, R., COLINI, L., NERI, M., BEHNCKE, B., SALVATORI, R., BUONGIORNO, M.F. and PARESCHI, M.T., 2009, Spectral properties of volcanic materials from hyperspectral field and satellite data compared with LiDAR data at Mt. Etna. *International Journal of Applied Earth Observation and Geoinformation*, **11**, pp. 142–155.

THONNARD, R.L.G., DENAYER, M.E. and ANTUN, P., 1965, *Carte Volcanologique des Virunga (1/50000)*, Afrique Centrale, Feuille No. 1, (Belgium: Centre National de Volcanologie).

TRUSDELL, F.A., 1995, Lava flow hazards and risk assessment on Mauna Loa volcano, Hawaii. In *Mauna Loa Revealed: Structure, Composition, History, and Hazards*, J.M. RHODES and J.P. LOCKWOOD (Eds.), pp. 315–336 (Washington, DC: American Geophysical Union, Geophysical Monograph, 92).

WIART, P.A.M., OPPENHEIMER, C. and FRANCIS, P., 2000, Eruptive history of Dubbi volcano, northeast Afar (Eritrea), revealed by optical and SAR image interpretation. *International Journal of Remote Sensing*, **21**, pp. 911–936.

Appendix A

Factor loadings for Landsat images used to map Nyamuragira lava flows (1967–2004). Those factor loadings displaying <6 PCs indicates either low spectral resolution scenes (e.g. 1974) or corrupted bands (e.g. 2003). The dark black outlines indicate the PCs chosen for unsupervised classification and the dark shaded cells represent the bands from the original imagery that contributed most to each PC. The PC combination used to map the individual flows are listed next to the flow year; those lightly shaded cells represent a deviation from PCs 1–3.

Imagery used-	4 December 1974			
Flow mapped: PCs used	1967: 1,2,3	1971: 1,2,3		
	PC1	**PC2**	**PC3**	**PC4**
B1	0.593	−1.889	0.625	−2.300
B2	0.257	−0.786	0.059	0.728
B3	0.078	0.008	−0.092	−0.011
B4	0.054	0.026	0.047	0.005

Imagery used-	7 August 1987					
Flow mapped: PCs used	1980: 1,2,3	1981: 2,3,4	1984: 1,2,4	1986: 1,2,3		
	PC1	**PC2**	**PC3**	**PC4**	**PC5**	**PC6**
B1	0.372	−1.028	−2.312	1.194	−1.163	−0.326
B2	0.356	−0.488	−0.963	−0.726	1.009	2.522
B3	0.190	−0.381	−0.330	−0.589	0.630	−0.648
B4	0.088	0.091	−0.030	−0.026	−0.018	−0.006
B5	0.065	−0.033	0.036	0.045	0.023	0.002
B7	0.021	−0.037	0.022	−0.047	−0.054	0.006

Imagery used-	17 January 1995					
Flow mapped: PCs used	1989a: 1,2,3	1994: 1,2,3				
	PC1	**PC2**	**PC3**	**PC4**	**PC5**	**PC6**
B1	0.921	−0.892	−0.469	1.495	0.430	−0.185
B2	0.350	−0.213	−0.283	−0.501	−0.065	−0.714
B3	0.125	−0.092	−0.047	−0.090	−0.119	0.181
B4	0.095	0.189	−0.120	0.008	0.039	0.029
B5	0.051	0.030	0.070	0.018	−0.042	−0.021
B7	0.028	−0.007	0.035	−0.028	0.067	0.016

Imagery used-	6 December 1999					
Flow mapped: PCs used	1989b,c: 1,2,3			1991: 1,2,3	1996a: 1,2,3	
	PC1	**PC2**	**PC3**	**PC4**	**PC5**	**PC6**
B1	0.576	1.145	−1.616	−0.811	2.732	0.395
B2	0.125	0.926	−1.035	−0.342	−1.382	1.757
B3	0.109	0.225	−0.182	0.046	−0.161	−0.351
B4	−0.057	−0.001	−0.025	0.017	0.003	−0.004
B5	−0.033	0.050	0.044	−0.045	0.000	−0.007
B7	0.008	0.049	0.032	0.076	0.016	0.020

Imagery used-	3 September 2000					
Flow mapped: PCs used	1996b: 1,2,4		2000b: 1,2,4			
	PC1	**PC2**	**PC3**	**PC4**	**PC5**	**PC6**
B1	0.974	−0.924	−0.492	0.085	1.675	0.606
B2	0.226	−0.116	−0.130	−0.027	−0.082	−0.416
B3	0.130	−0.085	−0.008	0.041	−0.173	0.128
B4	0.050	0.126	−0.117	−0.040	−0.004	0.032
B5	0.028	0.031	0.028	0.046	0.010	−0.007
B7	0.022	0.008	0.032	−0.039	0.003	0.002

Imagery used-	11 December 2001					
Flow mapped: PCs used	2000a: 1,2,3		2001a,b: 1,2,5			
	PC1	**PC2**	**PC3**	**PC4**	**PC5**	**PC6**
B1	0.621	1.522	−2.951	−3.824	3.332	−2.165
B2	0.004	0.742	−1.473	−0.429	−0.312	2.808
B3	0.102	0.220	−0.345	0.243	−0.299	−0.235
B4	−0.073	−0.030	−0.035	0.020	0.015	−0.006
B5	−0.058	0.062	0.034	−0.038	−0.037	−0.009
B7	−0.010	0.112	0.033	0.109	0.116	0.017

Imagery used-	31 January 2003		
Flow mapped: PCs used	2002a: 1,2,3		1998: 1,2,3
	PC1	**PC2**	**PC3**
B1	0.027	−3.979	−5.236
B2	0.164	−0.730	0.556
B3	−0.047	−0.007	0.005

Imagery used-	21 February 2005					
Flow mapped: PCs used	2002b: 1,2,3		2004: 1,2,3			
	PC1	**PC2**	**PC3**	**PC4**	**PC5**	**PC6**
B1	0.669	0.938	−2.859	3.886	2.246	1.551
B2	0.213	0.536	−1.604	0.047	−0.344	−2.992
B3	0.150	0.167	−0.399	−0.248	−0.399	0.297
B4	−0.068	−0.002	−0.023	−0.011	0.008	0.006
B5	−0.028	0.083	0.040	0.040	−0.043	−0.003
B7	0.016	0.076	0.003	−0.066	0.078	0.003

Appendix B

This flowchart describes, step-by-step, the processing routine we used to map Nyamuragira lava flows. We used ERDAS Imagine image processing software and ESRI ArcGIS software in our study, but these instructions can be translated to other image processing and mapping programs.